Renewable and Sustainable Energy Reviews 38 (2014) 1092–1099

Contents lists available at ScienceDirect

Renewable and Sustainable Energy Reviews

journal homepage: www.elsevier.com/locate/rser

The relationship between total solar radiation and biologically erythematic radiation over urban region of Egypt

Samy Abdelmordy Khalil [a,c,*], Ashraf Mustafa Shaffie [b,c]

[a] National Research Institute of Astronomy and Geophysics, Solar and Space Department, Marsed Street, Helwan, 11421 Cairo, Egypt
[b] Egyptian Meteorological Authority (EMA), P.O. Box 11784, Cairo, Egypt
[c] Department of Physics, Faculty of Science and Art, Qelwah, Al-Baha University, Kingdom Of Saudi Arabia

ARTICLE INFO

Article history:
Received 20 September 2012
Received in revised form
25 February 2014
Accepted 3 May 2014
Available online 27 June 2014

Keywords:
Stratosphere
Ozone layer
Biologically erythematic radiation
slant ozone
Scattering phenomena

ABSTRACT

This work studies the relationship between the effective of erythematic radiation (EER) and the total solar radiation (G) from urban region of Egypt. The measurements of total solar radiation (G) and biologically effective erythematic radiation (EER) incident on a horizontal surface at Cairo, Egypt (lat. 30°05′N and Long. 31°15′E), during the period time (1990–2010) are used. The relationship between hourly mean and daily mean of EER and the hourly mean daily mean totals of broadband total solar radiation is presented. The average hourly monthly mean variation of slant ozone Z and UVB transmission K_{tUVB} at the present work are found. The relation between the two variables slant ozone Z and UVB transmission K_{tUVB} show an opposite seasonal behavior, the low values of the slant ozone column during summer time produce high UVB transmission values in this season. The apposite pattern is observed during the winter. The Seasonal Statistical values of regression equations; the slopes (β), intercepts (α) and the standard errors (SE) for the fitted lines. The minimum slope occurs in winter, indicating that the percentage reduction in EER at higher SZA is larger than G. The variations of the slopes (β) during the course of the year ranges from a minimum of 0.2214 in winter to a maximum of 0.2914 in summer, the intercepts also show their minimum and maximum values in cold humid and hot dry months. The temporal variability of the percentage ratio of the total hourly mean daily erythema to total hourly mean daily broadband solar global irradiation (EER/G) is presented. The estimated values of UVB solar radiation a good agreement with the measured values of the UVB solar radiation, the difference between the estimated and measured values of UVB solar radiation varies from 2.3% to 3.6%.

Contents

1. Introduction

Stratospheric ozone is known to be the most important atmospheric factor determining clear sky UV-B radiation reaching the Earth's surface. The potential increase of UV-B exposure is the cause of mounting concern about the ozone layer. There are, however, other effects that influence the UV radiant energy transfer: cloud cover, aerosols, tropospheric ozone, and other gaseous pollutants. The relationships between various phenomena taking place in the atmosphere are complex and not well known. Therefore, ground based UV measurements are necessary to explore atmospheric changes and resultant effects on the biosphere. The spectral range of solar radiation corresponding to

* Corresponding author. Tel.: +20 225560645; fax: +20 225548020.
E-mail addresses: samynki@yahoo.com, samykhalil2014@gmail.com (S.A. Khalil), shaffie_2006@yahoo.com (A.M. Shaffie).

http://dx.doi.org/10.1016/j.rser.2014.05.014
1364-0321/

wavelengths $\lambda < 400$ nm, is called ultraviolet (UV). The ultraviolet is subdivided into three wavelength band regions: the UVA (315–400 nm) which is received at earth's surface, the UVB (280–315 nm) which is partially absorbed by ozone or scattered in the atmosphere and UVC (< 290 nm) which is potentially the most dangerous as it has the highest energy levels, but this wavelength band region is completely absorbed by stratospheric ozone and oxygen above about 30 km. The knowledge of solar UV radiation reaching the Earth's surface has a great interest because of its significant role in atmospheric and biological processes. The UV-B solar radiation (280–315 nm) represents less than 1% of the total radiation reaching the earth surface, and it is very important for the Earth-living systems because it is a radiation of high energy. UV-B irradiance on the Earth surface depends on geographical factors such as latitude, height, earth-sun distance, and solar zenith angle (SZA), etc. The influence of these factors can be evaluated using different radiative models. However UV-B solar radiation depends on atmospheric parameters like ozone, clouds and aerosols. Ozone is the gas that absorbs UV-C and some UV-B solar radiation and the effect of the total ozone column is included in all radiative models. Clouds are another attenuating factor of UV-B radiation and due to their random nature they are difficult to model. Aerosol is the factor that affects radiation levels under cloudless sky conditions [1–3].

During the last years, concerns about the intensity levels of UV-B radiation reaching the ground have increased due to the stratospheric ozone depletion and the dramatic increase in the number of skin cancers in the population. The UV solar irradiance at the ground varies greatly with local time, latitude and season, primarily because of the changing elevation of the sun in the sky. The ozone plays a role of shield around the Earth protecting us from ultraviolet radiation. The UVB radiation only represents 5% of the UV radiation [4], and 0.5% of the solar radiation, but UVB is very important to human beings because it can produce different illnesses [5]. Frequently the biologically effective irradiance is given as UV index (UVI). UVI is a dimensionless quantity and one unit is equivalent to 25 mW m^{-2} of erythematic radiation. The Earth's atmosphere significantly modifies the incoming solar radiation through the absorption and scattering process by gases, dust particles and other biosphere constituents of human and natural activities, there is clear linear correlation between UV-B total and global solar radiation, particularly in the region of moderate to low global irradiance, which enables estimation of UV-B flux in tropical/equatorial areas where facilities for UV-B measurements are not available, but global solar radiation flux data exist [3,6–9].

The relationship between total ozone and spectral UV irradiance from Brewer spectrophotometer observations and its use for derivation of total ozone from UV measurements has been the subject of [10]. The most significant influence on received clear sky UVB is that resulting from variation in atmospheric ozone [11]. Much of the harmful UV-B is absorbed by stratospheric ozone, although downward trends observed in total column ozone, particularly at high latitudes, and to a lesser extent at mid-latitudes, imply significant increase in the surface UV exposure [12]. The anticorrelation between total column ozone and UV radiation is a complex function of many variables, as: solar zenith angle, solar elevation, cloud cover, aerosol and vertical profile of ozone. The attenuation of UVB radiation by clouds is frequently larger than any other atmospheric parameter; however it is often only approximated by modeling the effect of monthly or seasonally averaged cloud amounts [13]. Ground-based observations can play an important role in improving the understanding of some of these effects [14,15].

The beneficial effects of UV-A and UV-B radiation on humans, the ecosystem, animals, plants, and materials have been addressed by many investigators [3,16–20]. The study of the ratios of biological UV to G have received a considerable attention in the past few years so that relationships of this type have been proposed by different investigators with measurements from Kuwait [21], Dharan [22], Edmonton [23], Saudi Arabia [24], Valencia [25,26], Spain [27,28], Egypt [29], France [30], Iran [31] and Switzerland [32]. In another study a relationship was established between an 18-month record of daily UV-B and full band (300–3000 nm) solar radiation in Sutton (England) [33]. They suggested a linear relation between the ratio of energy in the two wavebands and the cosine of zenith angle at noon time which enables the UV-B irradiation to be estimated from full band (G) solar radiation. Using a series of measurements including ultraviolet UV-B (280–320 nm), UV-A (320–400 nm), and broadband global (250–2800 nm) made from June 1998 to August 2001 at a station in Kwangju, South Korea, Ogunjobi and Kim [34] concluded that the ratio of total UV (280–400 nm) to broadband radiation is about 7.7% for all-sky conditions. The ratio of the ultraviolet to global radiation (UV/G) was also calculated by [19], for two cities in Egypt and compared with other sites in the Arabian Peninsula. Part of this study was used before to evaluate the prediction of clear-sky biologically effective erythematic radiation from global solar radiation [3].

In the present work, the estimation of hourly mean daily erythema (EER) from hourly mean daily broadband (G) in urban regions has rarely been studied, the main aim of this study is to establish an empirical relationship between total solar radiation (G) and effective erythema radiation (EER), which enables the estimation of the daily integrated EER from easily available broadband (250–2800 nm) G data in such climates, and the data in this study were obtained from the Meteorological Authority of Egypt.

2. Methodology and model variables

UVB measurements were converted into UVER (solar ultraviolet erythematic irradiance) values by means of conversion factors, (Diffey factor) provided by the manufacturer [35], and from them UVI (ultraviolet indices) hourly values were evaluated [36]. These UVI results have been considered as measured values and represented by (UVI) mean values (Middle East airlines values). UVI values have also been obtained from spectral calculated weighted by the erythema action spectrum, they are represented by (UVI) model and can be obtained by the following expression:

$$(\mathrm{UVI})_{\mathrm{model}} = K_{\mathrm{er}} \int_{290}^{400} E_{\lambda} S_{\mathrm{er}}\,(\lambda) d\lambda \tag{1}$$

Table 1
Monthly mean values of extraterrestrial solar radiation (Gmax.), long-term 1990–2010, total solar radiation (G) and air mass in noon time (m) at Cairo, Egypt.

Month	Jan.	Feb.	Mar.	Apr.	May	Jun.	Jul.	Aug.	Sep.	Oct.	Nov.	Dec.
$G_{max.}$ (Mj $^{m-2}$ d^{-1})	20.4	24.5	32.1	36.8	39.5	42.2	39.6	36.9	35.2	28.5	24.6	21.2
G (Mj $^{m-2}$ d^{-1})	12.8	14.9	16.8	19.5	25.3	27.6	26.4	24.2	21.6	19.3	14.9	13.7
m	1.47	1.31	1.15	1.06	1.03	1.01	1.04	1.06	1.11	1.18	1.31	1.42

Table 2
The average hourly monthly mean variation of slant ozone and UVB transmission at Cairo during the period from January 1990 to December 2010.

		1990	1991	1992	1993	1994	1995	1996	1997	1998	1999	2000	2001	2002	2003	2004	2005	2006	2007	2008	2009	2010
J	K_t	0.062	0.052	0.069	0.058	0.071	0.064	0.055	0.074	0.063	0.065	0.057	0.067	0.061	0.077	0.054	0.072	0.064	0.058	0.062	0.070	0.065
	Z	415	429	412	385	394	410	419	428	439	416	389	402	388	415	396	405	419	422	397	408	397
F	K_t	0.071	0.076	0.084	0.072	0.088	0.073	0.068	0.081	0.079	0.086	0.079	0.074	0.075	0.086	0.067	0.087	0.084	0.069	0.074	0.083	0.077
	Z	391	385	394	377	381	369	376	385	391	389	381	377	384	379	385	391	375	379	384	375	381
M	K_t	0.091	0.098	0.088	0.096	0.0104	0.0109	0.094	0.096	0.087	0.094	0.093	0.0104	0.0108	0.0101	0.097	0.091	0.095	0.096	0.094	0.097	0.092
	Z	342	355	348	339	357	345	351	357	339	344	357	349	338	358	350	341	345	338	347	342	348
A	K_t	0.112	0.117	0.0113	0.115	0.119	0.113	0.119	0.108	0.109	0.115	0.117	0.114	0.108	0.111	0.116	0.113	0.112	0.115	0.109	0.114	0.117
	Z	300	305	298	307	311	302	295	306	309	300	289	297	304	307	310	305	296	312	304	298	301
M	K_t	0.124	0.129	0.135	0.127	0.134	0.119	0.125	0.128	0.134	0.131	0.127	0.122	0.117	0.124	0.129	0.124	0.118	0.126	0.122	0.118	0.127
	Z	285	291	286	291	288	284	291	295	290	285	289	294	291	296	292	289	295	291	294	291	288
J	K_t	0.131	0.136	0.139	0.133	0.137	0.141	0.138	0.142	0.135	0.138	0.144	0.139	0.141	0.137	0.139	0.142	0.138	0.140	0.137	0.141	0.135
	Z	270	275	281	277	275	280	283	276	281	277	271	274	274	277	279	281	274	276	280	284	276
J	K_t	0.127	0.130	0.127	0.129	0.127	0.130	0.125	0.127	0.131	0.124	0.122	0.128	0.125	0.122	0.129	0.124	0.126	0.127	0.128	0.122	0.124
	Z	282	285	288	291	293	289	287	286	290	282	284	287	293	291	286	282	284	289	291	286	284
A	K_t	0.115	0.118	0.112	0.117	0.114	0.118	0.119	0.116	0.114	0.117	0.115	0.117	0.116	0.118	0.114	0.112	0.114	0.118	0.115	0.116	0.113
	Z	287	292	290	289	295	293	292	290	294	286	289	290	294	295	291	293	288	287	290	294	290
S	K_t	0.102	0.105	0.103	0.099	0.102	0.097	0.096	0.101	0.103	0.105	0.102	0.096	0.099	0.102	0.106	0.101	0.098	0.096	0.103	0.104	0.097
	Z	322	325	329	319	322	327	326	318	315	325	328	322	317	324	328	324	322	319	320	327	329
O	K_t	0.091	0.095	0.088	0.091	0.087	0.091	0.086	0.084	0.090	0.094	0.096	0.089	0.094	0.091	0.093	0.087	0.089	0.094	0.095	0.094	0.092
	Z	351	355	359	348	345	344	350	356	348	350	354	348	352	357	351	347	356	357	352	348	354
N	K_t	0.084	0.086	0.078	0.075	0.080	0.082	0.074	0.077	0.084	0.079	0.077	0.082	0.085	0.079	0.080	0.083	0.077	0.074	0.079	0.082	0.085
	Z	365	371	375	379	374	372	368	370	374	376	372	369	374	370	372	375	370	373	369	374	371
D	K_t	0.077	0.072	0.069	0.071	0.067	0.070	0.067	0.072	0.074	0.071	0.069	0.072	0.068	0.070	0.073	0.075	0.068	0.067	0.069	0.071	0.074
	Z	392	396	391	389	394	397	401	404	398	394	397	395	391	388	394	398	401	398	396	392	401

where K_{er} is $40\,m^2\,W^{-1}$, E_λ is the UV spectrum wavelength dependent ($Wm^{-2}\,nm^{-1}$) and K_{er} is the erythemal weighting function accepted by CIE (Commission International d'Eclairage) and given by [37].

The clearness index is chosen for characterizing jointly the cloud cover and aerosol load and it is evaluated by the following expression:

$$\mathrm{C.I.} = \left[\left\{\frac{(D_h+I_n)}{D_h}+KZ^3\right\}/\left\{1+KZ^3\right\}\right] \tag{2}$$

where D_h is the horizontal diffuse irradiance, I_n is the normal incidence direct irradiance, Z is the solar zenith angle and k is a constant whose value is 1.041 with Z in radians, by means expression (2), the dependence between the variable, C.I., and the solar zenith angle has been removed [38].

The slant total ozone column, Dobson (DU) represents the actual ozone amount in the atmosphere that the solar radiation passes through [39–41], have defined it as follows:

$$Z = \mathrm{TOC}/\mu \tag{3}$$

where μ is the cosine of the solar zenith angle, this expression is only valid for the direct solar irradiance. However, it can be used as a good approximation for the global solar irradiance (direct+ diffuse) since the largest part of ozone absorption occurs at high altitudes, before the scattering process by aerosol and cloud.

In analog with the broadband and UV cases, the UVB hemispherical transmittance can be defining in the following way [42,43].

$$K_{TUV} = \frac{\mathrm{UVB}}{\mathrm{UVBext.}} \tag{4}$$

where UVBext. is the extraterrestrial UVB radiation value on a horizontal surface it is given by

$$\mathrm{UVBext.} = I_{SCUVB}(12/\pi)\,E_0 \int_2^1 \sin(\theta)d \tag{5}$$

where (θ) is the solar elevation angle, E_0 is the correction factor for the eccentricity of the Earth's orbit, ω_i (i=1and 2) is the solar our angle at the beginning of period and at the end of period, respectively, and I_{SCUVB} is the UVB solar constant (21.51 W m^{-2}). It has been obtained from the spectral values given by [6,44].

The relationship between effective erythematic radiation (EER) and global solar radiation (G) as following Eq. (6) and several investigations [9,26,45,46], the linear relationship:

$$\mathrm{EER} = \beta G + \alpha \tag{6}$$

where EER is the daily erythem irradiance, G is the total daily broadband global radiation, β is the slope of the linear relation, and α is the intercept. Under clear-sky conditions, SZA and TCO appear to be the major determinant affecting the ratio of EER and G. Inverse relation is known between the ozone density in the atmosphere and the amount of UV reaching the earth's surface [47].

Other variables affecting by day-to-day fluctuation (aerosol, water vapor, air pressure) have smaller influence than SZA and TCO. In order to remove the ozone dependency from the relationship, the values of β were normalized to the 21-years (1990–2010) monthly mean climatological values of TCO using the following correction factor [48]:

$$C_{O_3} = \exp[-k_{O_3}\,(\Delta O_3)\,m_i] \tag{7}$$

where (ΔO_3) is the monthly mean difference between TCO in given month (i) and long-term climatological value, (m_i) is monthly mean air mass at noon time shows in Table 1, and (k_{O_3})=3.546 $(\mathrm{atm\,cm})^{-1}$ is the mean ozone absorption coefficient for the wavelengths 300–316 nm.

The Run-test were done on the daily observed data (EER and G) to make sure that the data are homogeneous and the variations of daily observed EER and G are caused only by climatic influences and not by other sources of errors (e.g. systematic errors caused by

Table 3
Means monthly and seasonal averages of the extraterrestrial UVB solar radiation, mesured and estímated UVB solar radiation and clearness index K_{tUVB} of UVB radiation at Cairo during the period 1990–2010.

Month	$UVB_{ext.}$ ($MJ\,m^{-2}\,h^{-1}$)	UVB ($MJ\,m^{-2}\,h^{-1}$)	$UVB_{est.}$ ($MJ\,m^{-2}\,h^{-1}$)	K_{tUVB}
Jan.	0.0755	0.0059	0.0042	0.071
Feb.	0.0774	0.0061	0.0055	0.082
Mar.	0.0816	0.0088	0.0072	0.101
Apr.	0.0828	0.0092	0.0086	0.118
May	0.0887	0.0107	0.0113	0.122
Jun.	0.0944	0.0125	0.0123	0.135
Jul.	0.0931	0.0133	0.0137	0.142
Aug.	0.0874	0.0121	0.0124	0.133
Sep.	0.0856	0.0100	0.0115	0.120
Oct.	0.0834	0.0087	0.0092	0.102
Nov.	0.0812	0.0068	0.0071	0.081
Dec.	0.0766	0.0052	0.0052	0.070
Winter	0.0782	0.0061	0.0065	0.084
Spring	0.0876	0.0114	0.0117	0.127
Summer	0.0883	0.0129	0.0128	0.134
Autumn	0.0809	0.0068	0.0071	0.084

Table 4
Climatological monthly means of meteorological parameters at Cairo during the period 1990 to 2010.

Month	Total column ozone (Dobson) (TCO)	Ratio of bright sunshine hours (n/N)	Total number of clear sky days (NCD)	Total number of dust days (NDD)	Relative humidity (RH %)
Jan.	291.5	0.638	17.2	1.4	52
Feb.	297.2	0.681	15.2	1.6	50
Mar.	288.4	0.647	13.5	2.7	48
Apr.	319.6	0.632	12.1	3.2	44
May	313.2	0.722	15.8	3.7	36
Jun.	306.4	0.857	25.4	3.5	32
Jul.	292.6	0.871	28.6	2.6	28
Aug.	295.3	0.834	29.7	2.4	24
Sep.	284.7	0.841	27.5	2.7	30
Oct.	282.2	0.759	25.4	2.9	39
Nov.	271.3	0.727	20.3	2.2	47
Dec.	295.4	0.659	18.3	1.4	61

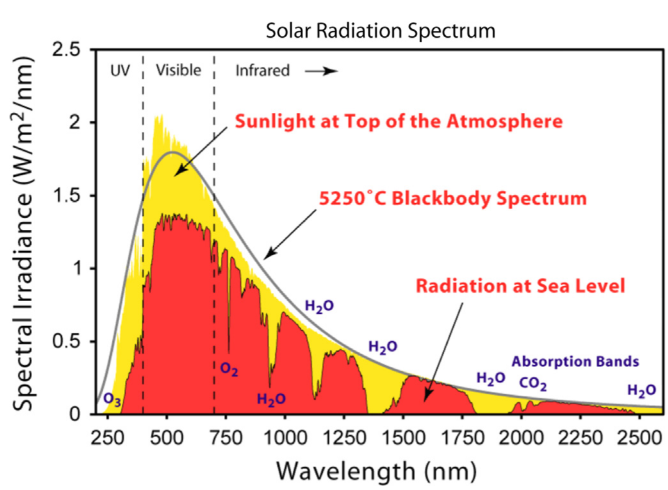

Fig. 1.

instruments; calibration problems; data transferring; etc.). These data are used to determine the temporal variability of the percentage ratio of the total daily erythema to total daily broadband solar global irradiation (EER/G). Note that, for calculating the annual cycle of the air mass (m) in Cairo, Egypt. The monthly mean solar zenith angle at noon time was used (Table 1). The analysis has been applied for clear-sky days when cloud amounts were less than two Oktas.

3. Results and discussion

Table 2, shows the average hourly monthly mean variation of slant ozone Z and UVB transmission K_{tUVB} at Cairo, Egypt during the period from January 1990 to December 2010. From this table, it is clear that the two variables show an opposite seasonal behavior, the low values of the slant ozone column during summer time produce high UVB transmission values in this season. The apposite pattern is observed during the winter. The average hourly monthly mean of slant ozone column and UVB transmission values shows the relationship between them in a clearer way than those of daily values. In winter months, UVB transmission values are low than those in summer months, this due to the fact that, the slant ozone column crossed by UVB radiation is higher in winter than in summer.

The mean monthly and the seasonal averages of the extra-terrestrial UVB solar radiation measured and estimated UVB solar radiation and clearness index K_{tUVB} of UVB radiation at Cairo during the period time 1990–2010 are listed in Table 3. From this table we notice that, the maximum values of the above parameters occur around the summer months, while the minimum values in winter months. But the values of these variables is clear that, in the spring and autumn months fall between the values of the summer and winter months. And also clear that from Table 3, the estimated values of UVB solar radiation a good agreement with the measured values of the UVB solar radiation. The difference between the estimated and measured values of UVB solar radiation varies from 2.3% to 3.6%. The average monthly UVB clearness index (K_{tUVB}) is less than corresponding values for global radiation k_t. Where the value of k_t is equal the value of global solar radiation (G) dividing by the value of extraterrestrial global solar radiation G_{ext}. However, the K_{tUVB} values vary from 0.070 to 0.142. This behavior is due to the extremely high attenuation of UVB radiation by stratospheric ozone and scattering phenomena.

The meteorological parameters (bright sunshine hours; relative humidity; total number of clear sky days; and total number of dusty days) have also been recorded during the present work (Table 4). To calculate the monthly mean values from the daily data, the work of Sabziparvar and Shetaee [48] was adapted. A dimensionless empirical relationship in the form of EER/G was developed, which can allow for the estimation of EER radiation from commonly measured global solar radiation (G). The daily clear-sky EER radiation can be estimated from broadband G data. Fig. 1–3 show the daily variability of clear-sky global solar radiation (G) and daily erythema radiation (EER), for the period of measurements. As seen, the daily EER is highly correlated with G, suggesting that daily EER doses can be obtained directly from G data. A linear regression line was fitted to the measured daily integrated G (as the independent variable) and daily EER (as the dependent variable). The regression analysis was applied to each season.

Table 5 performs the linear relations, the slopes (β), intercepts (α) and the standard errors (SE) for the fitted lines. As shown, the minimum slope occurs in winter, indicating that the percentage reduction in EER at higher SZA is larger than G. This can be explained by the increased ozone path length and higher percentage of scattering during the winter months.

In theory, the EER radiation must be zero when G is zero. As a result, the intercept (α) of the relations might be expected to be zero. In this study, it was not the case in Table 5. This can be explained by the uncertain relative behavior of EER and G under darkness conditions. Furthermore, when solar zenith angles are

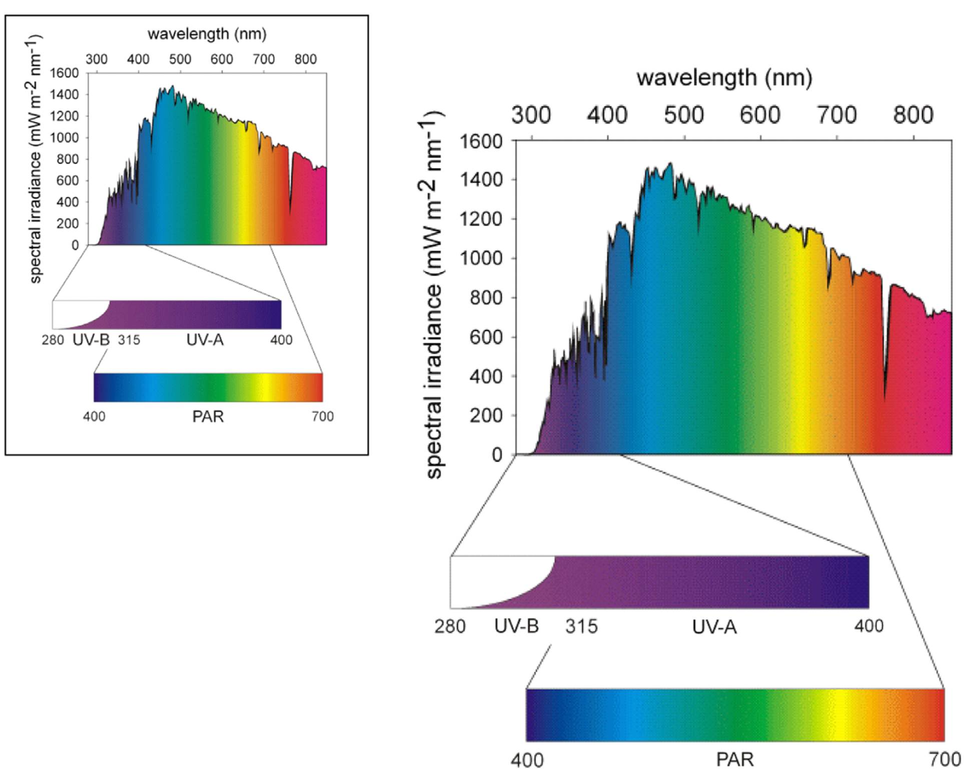

Fig. 2.

Fig. 3.

high (i.e. sunrise, sunset, winter months), the relative reduction in EER is disproportionately more than reduction in G because of the larger optical depths of ozone absorption and Rayleigh scattering.

As presented in Table 5, the variations of the slopes (β) during the course of the year ranges from a minimum of 0.2214 in winter to a maximum of 0.2914 in summer. The intercepts also show their minimum and maximum values in cold humid and hot dry months respectively. This result emphasis that the percentage reduction in the EER dose is always higher than such reduction in G when SZAs are high (i.e. winter). In addition to the seasonal relations, the following general relation was found to be reliable for estimation of daily integrated EER from global broadband solar radiation

Table 5
The seasonal statistical values of regression equations during the period of the present work (1990–2010).

Season	Effective erythema radiation of equation ($Kj\ m^{-2}\ d^{-1}$) ($EER = \beta G + \alpha$)	Standard error of the slop of equation SE (β) ($Kj\ m^{-2}\ d^{-1}$)	Standard error of the interception SE (α) ($Kj\ m^{-2}\ d^{-1}$)	Coefficient of determination (R^2)	Correction factor for the removal of ozone effect (C_{O_3})
Winter	$EER = 2.214 \times 10^{-1}$ G–0.685	±0.0137	±0.087	0.939	0.93
Spring	$EER = 2.845 \times 10^{-1}$ G–1.258	±0.0154	±0.154	0.885	0.96
Summer	$EER = 2.914 \times 10^{-1}$ G–2.332	±0.0124	±0.235	0.915	0.94
Autumn	$EER = 2.521 \times 10^{-1}$ G–2.185	±0.0081	±0.059	0.954	0.91

throughout the year:

$$EER\ (Kj\ m^{-2}\ d^{-1}) = 2.268 \times 10^{-1} G\ (Mj\ m^{-2}\ d^{-1}) - 2.411 \tag{8}$$

It should be reminded that other variables (aerosol, water vapor, and haze) affecting the two wave bands by day-to-day fluctuation, have a smaller influence than the annual SZA and TCO cycles. Additionally, the disproportional effects of the surface albedo and dust aerosols on EER and G, might explain some of the contradictions observed in the linear relations. Improved correlations and less dependence on location can be achieved by using longer period data at other latitudes and all weather conditions.

4. Conclusion

In this research we studies the average hourly monthly mean variation of slant ozone Z and UVB transmission K_{tUVB} at Cairo, Egypt during the period from January 1990 to December 2010. The two variables show an opposite seasonal behavior, the minimum values of the slant ozone column during summer time produce high UVB transmission values in this season. The apposite pattern is observed during the winter. The average hourly monthly mean of slant ozone column and UVB transmission values shows the relationship between them in a clearer way than those of daily values. In winter months, UVB transmission values are low than those in summer months, this due to the fact that, the slant ozone column crossed by UVB radiation is higher in winter than in summer.

The prediction values of UVB solar radiation a good agreement with the measured values of the UVB solar radiation, the difference between the prediction and measured values of UVB solar radiation varies from 2.3% to 3.6%. The Seasonal Statistical values of regression equations; the slopes (β), intercepts (α) and the standard errors (SE) for the fitted lines. As shown, the minimum slope occurs in winter, indicating that the percentage reduction in EER at higher SZA is larger than G. This can be explained by the increased ozone path length and higher percentage of scattering during the winter months. The variations of the slopes (β) during the course of the year ranges from a minimum of 0.2214 in winter to a maximum of 0.2914 in summer, the intercepts also show their minimum and maximum values in cold humid and hot dry months respectively. In general, the good relation was found to be reliable for estimation of daily integrated EER from global broadband solar radiation throughout the year as following:

$$EER\ (Kj\ m^{-2}\ d^{-1}) = 2.268 \times 10^{-1} G\ (Mj\ m^{-2}\ d^{-1}) - 2.411$$

References

[1] Palancar GG, Toselli BM. Effects of meteorology and troposphere aerosols on UV-B radiation: a 4-year study. Atmos Environ 2004;38:2749–57.
[2] Acosta LR, Evans WFJ. Design of the México City UV monitoring network: UV-B measurements at ground level in the urban environment. J Geophys Res 2000;105:5017–26.
[3] Khalil Samy A, Shaffie AM. Predication of clear-sky biologically effective erythematic radiation (EER) from global solar radiation (250–2800 nm) at Cairo. Egypt Adv Space Res 2013;51:1727–33.
[4] Miguel AH, Bilbao J, Salvador P. A study of UV total solar irradiation at a rural area of Spain, Solaris 2005 2nd Joint Conference, Athens (Greece), Hellenic Illumination Committee; 32–3, May 2005.
[5] Tevini M. In: Tevini Manfred, editor. Molecular biological effects of ultraviolet radiation. UV-B radiation and ozone depletion: effects on humans, animals, plants, microorganism, and materials. Lewish Publishers; 1993. p. 1–17.
[6] Iqbal M. An introduction to solar radiation. New York: Academic Press; 1983; 390.
[7] Ilyas M, pandy A, Hassan SIS. UV-B radiation at Penang. Atmos Res 1999;51: 141–52.
[8] Koronakis PS, Sfantos GK, Plaiatsos AG, Kaldellis JK, Garofalakis JE, Koronaki IP. Interrelations of UV-global/global/diffuse solar irradiance components and UV-global attenuation on air pollution episode days in Athens, Greece. Atmos Environ 2002;36:3173–81.
[9] Korany MH, Basset HA. The global and UV-radiation over Egypt. Atmosphere 2007;20(4):341–58.
[10] Fioletov VE, Kerr JB, Wardle DI. The relationship between total ozone and spectral UV irradiance from Brewer spectrophotometer observations and its use for derivation of total ozone from UV measurements. J Geophys Res Lett 1997;24:2705–8.
[11] Frederick JE, Koob AE, Alberts AD, Weatherhead EC. Emperical studies of tropospheric transmission in the ultraviolet: broadband measurements. J Appl Meteor 1993;32:1883–92.
[12] Herman JR, Brahma PK, Ziembke J, Ahmad Z, Larks D. UV-B increases (1979–1992) from decreases in total ozone. Geophys Res Lett 1996;23:2117–20.
[13] Frederick JE, Snell HE. Tropospheric influence on solar ultraviolet radiation: the role of clouds. J Clim 1990;3:373–81.
[14] Madronich S. Implications of recent total atmospheric ozone measurements for biologically active ultraviolet radiation reaching the Earth's surface. J Geophys Res Lett 1992;19:37–40.
[15] Madronich S, Flocke S. Theoretical estimation of biologically UV radiation at the Earth's surface. In: Zerefos CS, Bais AF, editors. Solar Ultraviolet Radiation Modeling, Measurements and Effects, vol. 52. Berlin: NATOASI Series, Springer; 1997. p. 23–48.
[16] Webb AR. Who, what, where and when influences on cutaneous vitamin D synthesis. Prog Biophys Mol Biol 2006;92(1):17–25.
[17] McKinlay AF, Diffey BL. A reference action spectrum for ultraviolet induced erythemal in human skin. CIE-Hirek 1987;6:17–22.
[18] Som AK. Solar UV-B radiation measurements over Bahrain. Renew Energy 1992;2(1):93–8.
[19] Robaa SM. A study of ultraviolet solar radiation at Cairo urban area, Egypt. Sol Energy 2004;77:251–9.
[20] Sabziparvar AA, Shine KP, Forster PM de F. A model-derived global climatology of UV irradiation at the Earth's surface. J Photochem Photobiol 1999;69 (2):193–202.
[21] Al-Aruri SD. The empirical relationship between global radiation and global ultraviolet (0.290–0.385) μm solar radiation components. Sol Energy 1990;45:61–4.
[22] Elhadidy MA, Abdel-Nabi DY, Kruss PD. Ultraviolet solar radiation at Dhahran, Saudi Arabia. Sol Energy 1990;44:315–9.
[23] Sadler GW. Ultraviolet radiation at Edmonton, Alberta, Canada. Sol Energy 1992;49:13–7.
[24] Mujahid AM. Correlation between ultraviolet radiation and global radiation in Riyadh, Saudi Arabia. J Sol Energy Eng Trans ASME 1994;116(1):63–6.
[25] Martinez-Lozano JA, Casanovas AJ, Utrillas MP. Comparison of global ultraviolet (290–385 nm) and global irradiation measured during the warm season in Valencia, Spain. Int J Climatol 1994;14:93–102.
[26] Martinez-Lozano JA, Tena F, Utrillas MP. Ratio of UV to global broad band irradiation in Valencia, Spain. Int J Climatol 1999;19:903–11.
[27] Foyo-Moreno I, Vida J, Alados-Arboledas L. Ground based ultraviolet (290–385 nm) and broadband solar radiation measurements in south-eastern Spain. Int J Climatol 1998;18:1389–400.
[28] Foyo-Moreno I, Vida J, Alados-Arboledas L. A simple all weather model to estimate ultraviolet solar radiation (290–385 nm). J Appl Meteorol 1998;38:1020–5.
[29] Trabea AA, Salem AI. Empirical relationship for ultraviolet solar radiation over Egypt. Egypt J Sol Energy 2001;24:123–32.
[30] De La Casinière A, Touré ML, Masserot D, Cabot T, Pinedo Vega JL. Daily doses of biologically active UV radiation retrieved from commonly available parameters. Photochem Photobiol 2002;76(2):171–5.

[31] Sabziparvar A. An improved estimation of daily clear-sky biologically EER from broadband global solar radiation, Inter. J Biometeorol 2009;53:239–45.
[32] Lindfors A, Vuilleumier L. Ryythemal UV at Davos (Switzerland), 1926–2003, estimated using total ozone sunshine duration, and snow depth. J Geophys Res D: Atmos 2007;110:1–15.
[33] Webb A, Steven MD. Daily total of solar UV-B radiation estimated from routine meteorological measurements. J Climatol 1986;6:405–11.
[34] Ogunjobi KO, Kim YJ. Ultraviolet, (0.280–0.400 mm) and broadband solar hourly radiation at Kwangju, South Korea: analysis of their correlation with aerosol optical depth and clearness index. Atmos Res 2004;71:193–214.
[35] S.I.R.S.A. Manual de usuario, Sensor de radiación ultraviolet, modelo UVB-1; 1998 ⟨sirsa@sirsa.es⟩.
[36] WMO, Report of the WMO meeting of experts on UV-B measurements, data quality and standardization of UV indices, Les Diablerets, Switzerland; 1994.
[37] McKinlay AF, Diffey BL. A reference action spectrum for ultraviolet induced erytema in human skin. CIE J 1987;6:17–22.
[38] Perez R, Ineichen P, Seals R. Modeling daylight availability and irradiance components from direct and global irradiance. Sol Energy 1990;44(5):271–89.
[39] Anton M, Serrano A, Cancillo ML, Garcia JA. An empirical model to estimate ultraviolet erythemal transmissivity. Ann Geophys 2009;27:1387–98.
[40] Serrano A, Anton M, Cancillo ML, Garcia JA. Proposal of a new erythemal UV radiation amplification factor. Atmos Chem Phys Discuss 2008;8:1089–111.
[41] Anton M, Serrann A, Cancillo M, Garica JA. An empirical model to estimate ultraviolet erythemal transmissivity. Ann Geophys 2009;27:1387–98.
[42] Kudish AI, Lyubansky V, Evseev EG, Ianetz A. Intercomparison of the solar UVB, UVA and global radiation clearness and UV indices for Beer Sheva and Neve Zohar (Dead Sea), Israel. Energy 2005;30:1623–41.
[43] El-Nouby Adam M. Effect of stratospheric ozone in UVB solar radiation reaching the Earth's surface at Qena. Egypt Atmos Pollut Res 2010;1:155–60.
[44] El-Nouby Adam M. effect of the atmosphere on UVB radiation reaching the earth's surface: dependence on solar zenith angle. Atmos Oceanic Sci Lett 2011;4(3):139–45.
[45] Krzyscin JW, Jaroslawski J, Sobolewski PS. Effects of clouds on the surface erythemal UV-B irradiance at northern midlatitudes: estimation from the observations taken at Belski, Poland (1999–2001). J Atmos Sol—Terr Phys 2003;65:457–67.
[46] Canada J, Pedros G, Bosca JV. Relationships between UV (0.290–0.385 mm) and broadband solar radiation hourly values in Valencia and Cordoba, Spain. Energy 2003;28:199–217.
[47] Zerefos C, Balis D, Tzortziou M, Bais A, Tourpail K, Meleti C, et al. A note on the interannual variations of UV-B erythemal doses and solar irradiance from ground-based and satellite observations. Ann Geophys 2001;19(1):115–20.
[48] Sabziparvar A, Shetaee H. Estimation of global solar radiation in arid and semi-arid climates of East and West Iran. Energy 2007;32(5):649–55.